Oil Shale, 2020, Vol. 37, No. 4, pp. 319–333
doi: https://doi.org/10.3176/oil.2020.4.05
ISSN 0208-189X

Evaluation of the porosity and permeability of oil shale during in-situ conversion process through numerical simulation and mathematical modeling

Atif Zafar[a,b], Yuliang Su[a]*, Wendong Wang[a], Muhammad Kashif[c], Asif Mehmood[a], Syed Ghufran Alam[b]

[a] School of Petroleum Engineering, China University of Petroleum (East China), 266580, Qingdao, China
[b] Department of Petroleum Technology, University of Karachi, University Road, 75270, Karachi, Pakistan
[c] Department of Earth Sciences, University of Sargodha, Sargodha, 40100, Pakistan

Abstract. *In this paper a simulation model of oil shale formation is generated in which the reservoir is heated by downhole heaters and subsurface solid kerogen is converted into liquid and gas hydrocarbons by the function of chemical reactions, temperature and time. On the basis of the results obtained, the alteration in porosity and permeability is evaluated. It is found that the porosity and permeability of oil shale increase significantly as a function of in-situ kerogen conversion into oil and gas. A new mathematical modeling approach is adopted to measure the quantitative change in porosity. It is revealed that the effective porosity of the studied reservoir increases from the initial value of 5% to the final value of 12.5% after in-situ kerogen pyrolysis. In-situ permeability, as a function of porosity, is also modeled and a noteworthy increase is observed. The results are compared with previously published experimental findings and are found to be in a good agreement.*

Keywords: *in-situ pyrolysis, kerogen conversion, oil shale, permeability, porosity.*

1. Introduction

Oil shale is a sedimentary rock that contains a noteworthy quantity of kerogen, which is the source of generating hydrocarbon as oil and gas [1]. Oil shale reserves are found in many regions of the world [2]. As per precise estimation, the worldwide reserves of oil shale are around 3.6×10^{11} m^3 [3]. But the major reserve holder region is the United States of America having approximately total oil shale reserves around 1.8×10^{11} m^3 [3]. Based on these numbers, oil

* Corresponding author: e-mail *suyuliang@upc.edu.cn*

shale may be a significant alternative fuel resource in upcoming decades.

The kerogen in oil shale is found as a solid phase and can be converted into liquid and gas-phase hydrocarbons by different methods, i.e. ex-situ and in-situ retorting or pyrolysis of this organic material. The ex-situ pyrolysis is carried out at the surface in a wide range of temperature by mining the oil shale rock from the subsurface, but this method has numerous limitations, of which two are major ones, i.e. depth of oil shale reservoir and environmental issues [4].

In-situ pyrolysis of oil shale includes subsurface heating of the reservoir. The heating process can be carried out by different methods, i.e. electrical or non-electrical [5]. Applied in a field in Colorado, Shell's in-situ electrical heating pilot project proved to be successful, opening new windows for research into this method [5]. Although the in-situ pyrolysis method has many advantages over ex-situ process such as no excretion of environmentally hazardous and poisonous water and gases, and a comparatively high technical feasibility for deeper oil shale reservoirs, the main hindrance to adopting this method is economics, because in-situ heating requires a significant amount of direct or indirect input of energy [6–8].

Normally, the initial porosity and permeability of oil shale are very low so that any fluid may not flow through it without application of a stimulation technique [9–13]. When the shale formation is heated, the kerogen which exists as a solid phase is converted to hydrocarbon and other fluids, ultimately increasing the void pores in the rock. These void pores increase the effective porosity of oil shale which translates to positive alteration in permeability.

Some researchers conducted studies on conversion, fluid flow and production process of oil shale, i.e. implemented Steamfrac for in-situ conversion process (ICP) [14], in which they modeled the conversion process of oil shale by steam injection through hydraulic fractures. Some investigators compared different methods of in-situ upgrading in terms of energy efficiency [15], while some worked on different aspects and impacts of chemical reactions [16]. Experiments with oil shale from Shell's Mahogany oil shale field were also simulated [17]. The results of another Shell-run pilot project of oil shale ICP were also modeled [18]. But all those researchers did not consider the dynamic properties alteration like change in porosity and permeability which occurs at every moment of the in-situ upgrading of an oil shale reservoir.

In the numerical simulation of in-situ pyrolysis, many complicated processes need to be incorporated, i.e. heat flow through conduction and convection, kerogen conversion, chemical reactions, fluid flow, and production. There have been carried out rare studies to develop a simulator to incorporate the whole in-situ conversion process of an oil shale reservoir. Some investigators worked on modeling the fronts of chemical reactions and heat dissipation [19], while others developed a model to incorporate the hot CO_2 injection based on non-dimensional equations, assuming no effects of

temperature on reaction rate [20]. Some scientists developed a simulator and studied the sensitivity of Shell-tested in-situ conversion process [5], whereas some researchers developed a simulator only for kerogen conversion [21]. However, all those studies ignored the effect of kerogen pyrolysis on porosity.

Since the alteration mechanism of effective porosity and permeability is a key parameter in the in-situ upgrading of oil shale, therefore, it should be more focused on further research within this domain. It is because the change in porosity is directly and change in permeability is indirectly related to kerogen decomposition which occurs at every time step [22–26]. Hence the acknowledgment of alteration in porosity and permeability during in-situ conversion process is essential to correctly model the dynamics of fluid flow, heat flow, and chemical reactions as well. Therefore, in this study, a dual permeability oil shale reservoir numerical simulation model is generated using a commercial reservoir simulator having thermal and compositional modeling options. Simple chemical reactions were established and the in-situ heating and pyrolysis of kerogen, said chemical reactions, and fluid and heat flow were simulated. Kerogen consumption was investigated accordingly through simulation and on the basis of this a mathematical correlation for porosity evaluation was established. Since permeability is dependent on porosity, therefore, the incremental permeability was also estimated by the Carmen-Kozeny model. This technique will help overcome challenges of in-situ upgrading of oil shale. Figure 1 shows the physical connotation of the concept of this study.

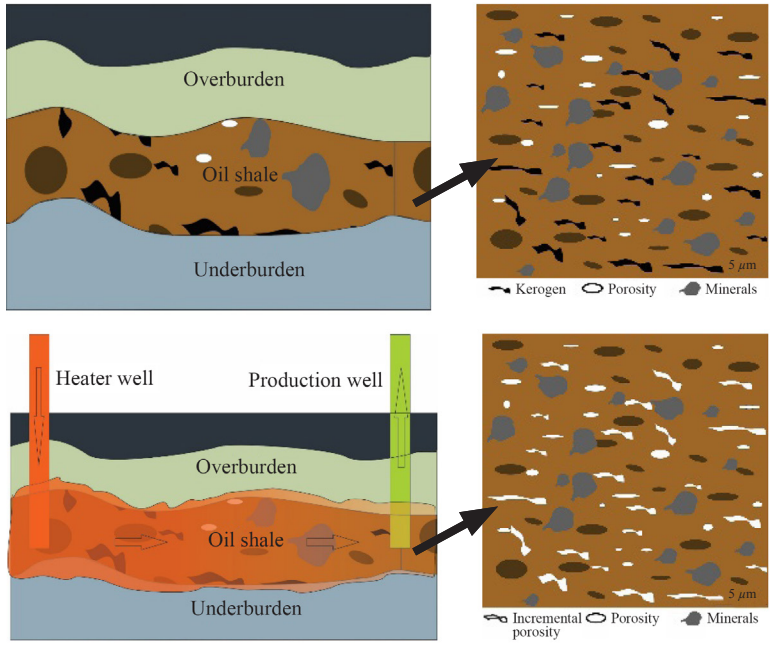

Fig. 1. A conceptual model of incremental porosity of oil shale during in-situ conversion process on the basis of kerogen consumption.

2. Numerical simulation

2.1. Numerical model description

A dual permeability oil shale reservoir model was generated on a commercial simulator by assuming the thickness and depth of the formation to be 36 m and 61 m, respectively. The Cartesian Grids were modeled as 9 × 9 × 28 number of blocks with 0.44 m × 0.44 m × 3 m dimensions like a square well pattern having four heater wells with the spacing of 3.96 m and one production well in the middle (Fig. 2).

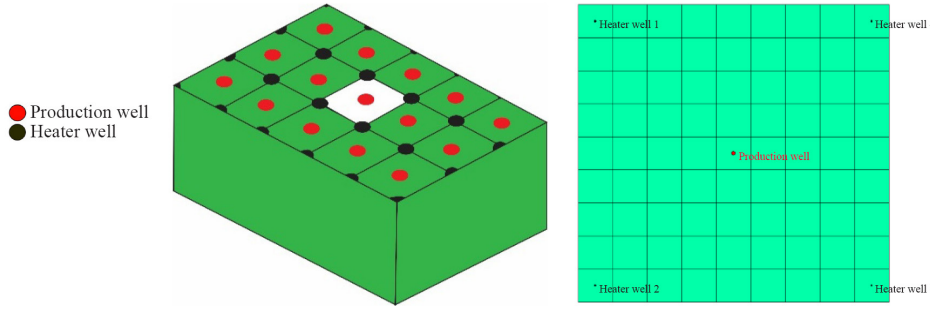

Fig. 2. Well pattern used in the study.

The values of reservoir pressure, depth, net pay and matrix effective porosity were taken from the Mahogany Demonstration Project (MDP), a pilot project of in-situ pyrolysis of oil shale. Shell, the operator of MDP, conducted this project from the year 2003 to 2005. The geological formation was Green River. In MDP sixteen heater wells were drilled in three circles while two production wells were drilled in the center [5]. In most of the previous researches regarding ICP, fractures were not included in the model. In our model, natural fractures were also considered with a fracture spacing (FS) of 1 m in the base case as shown in Table 1. The other reservoir properties used in our model, such as matrix effective porosity and permeability, were adopted as per within the range of already published oil shale data and are summarized in Table 1 [9, 14]. Oil shale has a very low initial porosity and permeability; therefore, the values were taken as 0.05 md fraction for initial effective porosity and 0.02 md for matrix permeability in horizontal direction. To acknowledge the permeability anisotropy, the vertical matrix permeability was taken as 0.002 md whereas oil shale formation compressibility was taken as 4.35×10^{-7} 1/kPa (Table 1).

Table 1. Reservoir properties used in the study

Parameter	Value	Unit
Reservoir pressure	700	kPa
Reservoir depth	600	m
Reservoir net pay	36	m
Fracture spacing	1	m
Matrix effective porosity	0.05	Fractions
Fracture porosity	0.8	Fractions
Matrix permeability, horizontal	0.02	md
Matrix permeability, vertical	0.002	md
Fracture permeability, horizontal	100	md
Fracture permeability, vertical	10	md
Initial kerogen content	20000	$gmol/m^3$
Density of oil shale	2	gm/cm^3
Formation compressibility	4.35×10^{-7}	1/kPa
Initial reservoir temperature	28	ºC
Heater wells temperature	340	ºC

For the simplicity of the chemical model and to minimize the processing time of compositional and thermal simulation, normally the least number of components is used. For this purpose, a larger number of components is lumped (pseudoized) into a smaller number to define the fluid volumetric and phase behavior through an equation of estate (EOS). In this study, a fluid model, with hydrocarbon pseudo-component lumping and pressure-volume-temperature (PVT) properties, was generated through WINPROP software which is a module of the main simulation software used. The fluid model consisted of three generic pseudo-components, namely heavy oil, light oil and gas, which were lumped through the user-defined lumping scheme as shown in Table 2. The lumping process of the components consisted in mapping the 45 hydrocarbon species into three generic pseudo-components. The actual hydrocarbon components through C_{21} to C_{45}, C_6 to C_{20} and C_1 to C_5 were lumped to pseudo-components heavy oil, light oil and gas, respectively. Lee and Kesler mixing rules were applied to calculate the critical properties of the pseudo-components.

Table 2. Properties and composition of the lumped components

Lumped component	Hydrocarbon pseudo-component range	Critical pressure, kPa	Critical temperature, °C	Molecular weight, g/mol	Acentric factor
Heavy oil	C_{21}–C_{45}	1199.18	562.42	341.2	0.969
Light oil	C_6–C_{20}	2320.88	374.94	157	0.492
Gas	C_1–C_5	4541.86	38.73	34.07	0.095

Temperature-dependent kerogen conversion chemical reactions were established by modifying the reaction model offered by Fan et al. [5]. The slightly modified chemical reactions and relevant kinetic data are given in Table 3. Water and CO_2 were eliminated from the reactions while prechar was considered as part of the remaining solid phase. In fact, this modification did not affect the rate of production [5].

Table 3. **Chemical reactions model (modified after [5])**

No.	Reaction	Activation energy, J/mol	Frequency factor
1	Kerogen → 0.0107 heavy oil + 0.0097 light oil + 0.0072 hydrocarbon gas	213500	2.59×10^{18}
2	Heavy oil → 0.6613 light oil + 1.5038 hydrocarbon gas	226090	8.64×10^{17}
3	Light oil → 3.2378 hydrocarbon gas	226090	4.32×10^{16}

3. Mathematical models for altered porosity and permeability

Kerogen exists as a solid phase in the pores of oil shale formation and decomposes by in-situ pyrolysis process which results in the change of void space volume. The incremental porosity (φ_{inc}) during in-situ pyrolysis together with the initial effective porosity (φ_{IE}) of oil shale formation makes the total altered porosity (φ_{TA}), as shown in Equation (1):

$$\varphi_{TA} = \varphi_{IE} + \varphi_{inc}. \quad (1)$$

As per the basic definition, porosity *(φ)* is the ratio of the pore volume (V_p) to the bulk volume volume (V_b) of the rock as shown in Equation (2):

$$\varphi = \frac{V_p}{V_b}. \tag{2}$$

Note that in the case of oil shale, the pore volume (V_p') also contains the solid phase kerogen (V_k):

$$V_p^{'} = V_p - V_k. \tag{3}$$

After in-situ pyrolysis, this solid-phase kerogen (V_k) was converted to fluid by creating more void pores. Therefore, Equation (2) can be written as:

$$\varphi_{inc} = \frac{V_p - V_k}{V_b}, \tag{4}$$

$$\varphi_{inc} = \frac{V_p}{V_b} - \frac{V_k}{V_b}. \tag{5}$$

Since the incremental porosity belongs to the portion of no-fluid porosity or, in other words, void porosity (φ_v) and the ratio of kerogen concentration to bulk volume also belongs to void porosity, therefore, Equation (5) can be written as:

$$\varphi_{inc} = \varphi_v - \varphi_v \left[\frac{k_{con}}{k_\rho}\right], \tag{6}$$

$$\varphi_{inc} = \varphi_v \left[1 - \frac{k_{con}}{k_\rho}\right], \tag{7}$$

where k_{con} is the concentration and k_ρ is the density of kerogen at the pore level. So, Equation (1) can be written as:

$$\varphi_{TA} = \varphi_{IE} + \varphi_v \left[1 - \frac{k_{con}}{k_\rho}\right]. \tag{8}$$

The above equation can be used to find out the total altered porosity at any time step as the function of kerogen concentration. For the altered permeability *(K)*, the Carmen-Kozeny model (Eq. (9)) was used utilizing the values of known initial permeability (K_0) and total altered porosity (φ_{TA}) obtained from Equation (8):

$$K = K_0 \times \left[\frac{\varphi_{TA}}{\varphi_{IE}}\right]^3 \times \left[\frac{1 - \varphi_{IE}}{1 - \varphi_{TA}}\right]^2. \tag{9}$$

4. Results and discussion

4.1. Base case scenario

Since the in-situ kerogen conversion rates are dependent on temperature, therefore, the subsurface heating of the oil shale formation was achieved by four downhole heater wells at a constant temperature of 340 °C, started from the very first day of simulation. The heat started to dissipate into the reservoir and it took approximately 386 days for the temperature of the whole simulated section of the reservoir to reach 340 °C. This is illustrated in Figure 3a which shows the temperature distribution in the reservoir at different time periods.

Due to the continuous subsurface heating, kerogen decomposed and hydrocarbon was generated as per the established chemical reactions. It can be seen from Figure 3b that kerogen started to decompose first from near the heater well region and was then depleted in the whole simulation section accordingly. This occurred because the kerogen conversion process was dependent on temperature. At the end of 386 days almost all the kerogen was converted. As seen from Figures 3a and 3b, heat affected the upper and lowest zones of the reservoir differently from its whole middle part. This happened due to the heat losses of overburden (OB) and underburden (UB) geological formation.

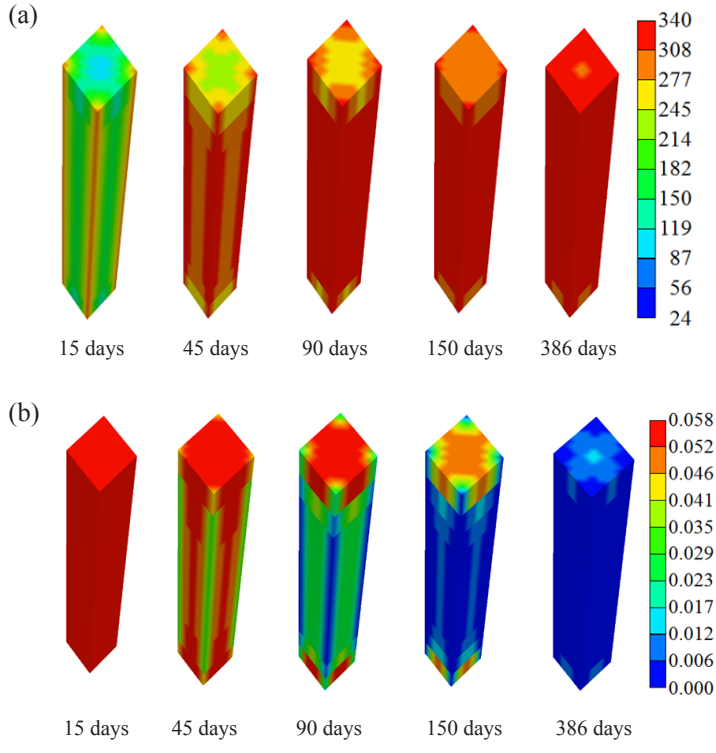

Fig. 3. (a) Distribution of temperature after 15, 45, 90, 150 and 386 days; (b) distribution of kerogen (fraction) after 15, 45, 90, 150 and 386 days.

Due to the elevated temperature kerogen was converted to hydrocarbons. Then these hydrocarbons (liquid and gas) were produced through the production well. Figure 4a demonstrates the oil and gas production rate at surface condition (SC) as per the function of temperature and also shows some typical characteristics of ICP. The figure reveals that the production rate of gas was high at the initial stage of the process. There were two reasons for this. First, the quantity of the gas phase already present in the effective porosity and the fractures moved first. Second, since the heaters were operated at a high temperature (340 °C), the kerogen conversion took place very quickly in the heater blocks.

The peak of hydrocarbon production was achieved by the 90th day after which the rate decreased gradually. Figure 4b shows the cumulative oil and gas production and cumulative kerogen consumption. It can be seen from the figure that the cumulative oil and gas production is totally dependent on kerogen consumption.

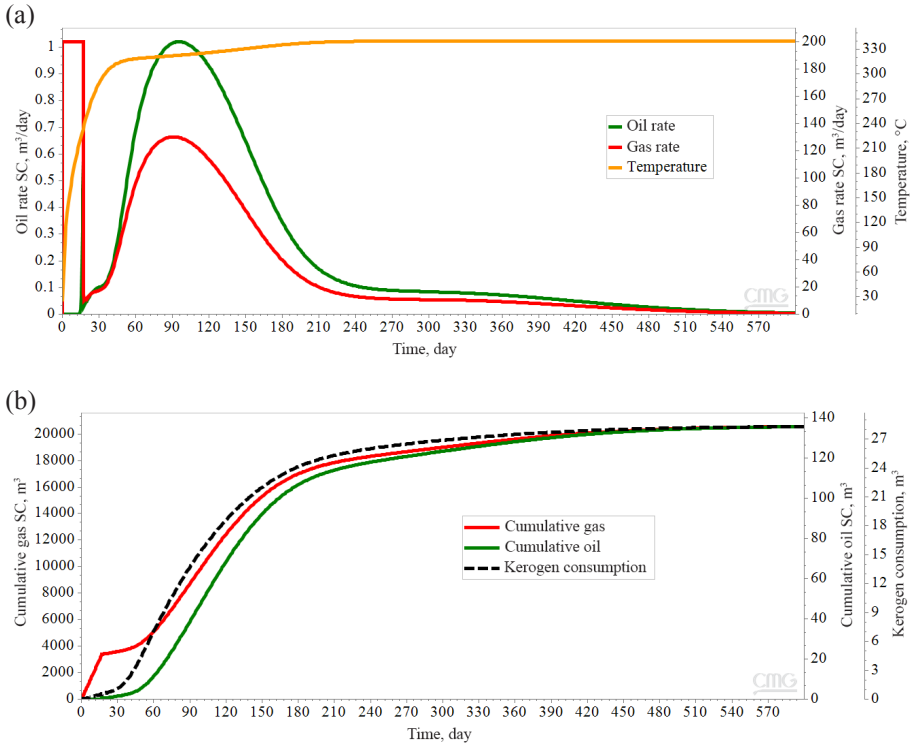

Fig. 4. (a) Temperature distribution and oil and gas rate; (b) cumulative oil and gas production and kerogen consumption.

On the basis of the kerogen consumption which was estimated through numerical simulation, the altered porosity was evaluated using the proposed model (Eq. (8)). Since permeability is dependent on porosity, therefore, the altered permeability was also computed using the Carmen-Kozeny model (Eq. (9)). Figure 5 shows the change of initial porosity and permeability as a function of kerogen consumption during the in-situ pyrolysis process of kerogen of oil shale. It can be observed that the porosity increased significantly from the initial value of 5% to the final value of 10.2% whereas permeability was also increased from 0.02 md to 0.19 md in the base case scenario.

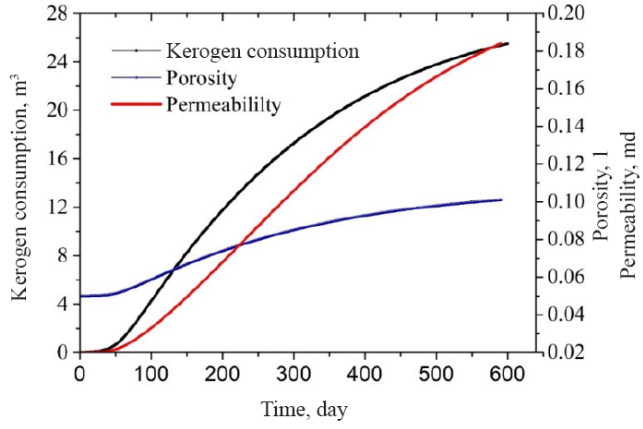

Fig. 5. Altered porosity and permeability as a function of kerogen consumption.

4.2. Sensitivity study

Two parameters of the numerical reservoir simulation model, i.e. the initial kerogen concentration and fracture spacing, were selected to run different sensitivities. Then the values of kerogen consumption obtained in these sensitivity studies were estimated through numerical simulation. On the basis of the obtained kerogen consumption values, the different trends of incremental porosity were evaluated through the mathematical model proposed by us (Eq. (8)), whereas the values of incremental permeability were also estimated through the Carmen-Kozeny model (Eq. (9)) by using said trends.

The main reason behind selecting these two parameters for sensitivities is that they are not fixed, i.e. they have not been reported previously. But there are some predefined reasonable ranges of these parameters found in literature. For example, Dyni [3] offered a range of the initial concentration of kerogen from 10 to 20 wt% for the commercial feasibility of oil shale. This range translates to 0.2 to 0.4 g kerogen/cm^3 as the density of kerogen in oil shale (since oil shale has a density of approximately 2 g/cm^3). So, as per the chemical formula of kerogen, these values correspond to the range of 13615 to 27231 gmol/m^3 [5].

Therefore, the three scenarios of the initial concentration of kerogen were taken as higher (27000 gmol/m^3), medium (20000 gmol/m^3) and lower (13000 gmol/m^3) for the input of numerical simulation. On the basis of the results of those sensitivity studies, the incremental values of porosity and permeability were evaluated, as shown in Figure 6a. The figure displays that porosity was increased from 5 to 12.5% at a higher initial concentration of kerogen while the increment was 5 to 10% and 5 to 8% for the medium and lower kerogen concentration, respectively. The same trend was also observed for the incremental permeability. So, it was shown that the higher the initial concentration of kerogen, the greater the change in porosity. As a

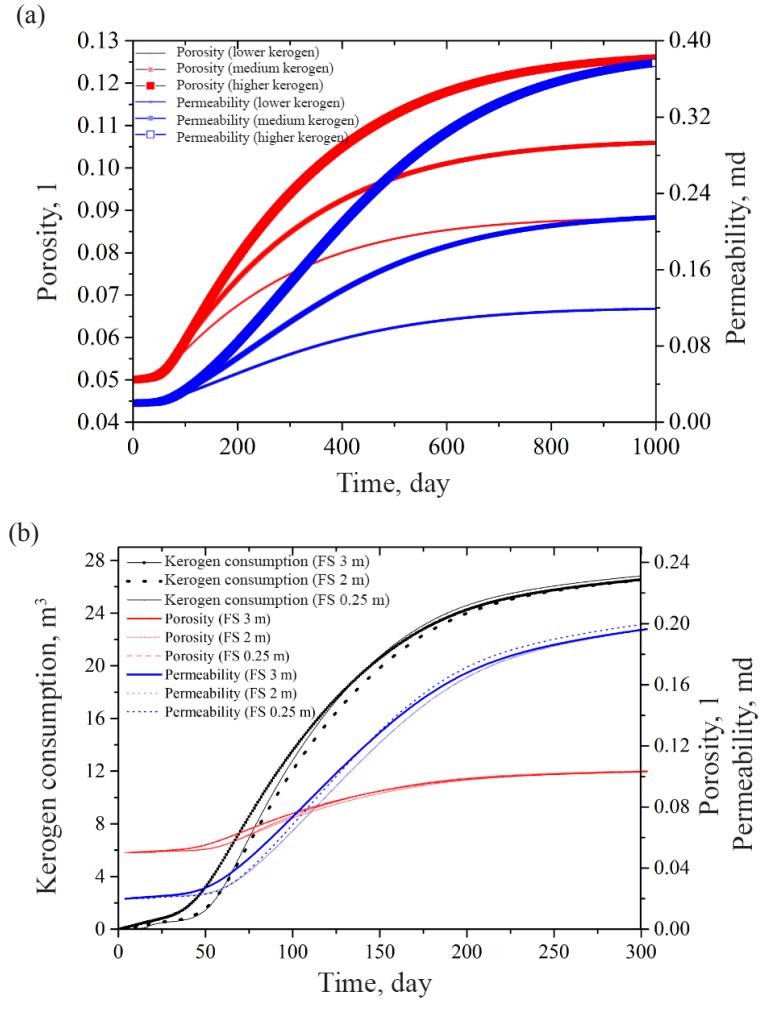

Fig. 6. (a) Altered porosity and permeability at different initial kerogen concentrations; (b) altered porosity and permeability, and kerogen consumption at different fracture spacings (FS).

result, the higher incremental permeability will be achieved at a higher initial concentration of kerogen.

The three scenarios of fracture spacing were taken as 0.25 m, 2 m and 3 m for the input of numerical simulation. On the basis of the results of those sensitivity studies, the incremental values of porosity and permeability were evaluated, as shown in Figure 6b. The figure demonstrates that different values of fracture spacing did not affect the increasing trend of porosity. Although there was a certain increment in the final value of permeability, from 0.19 to 0.2 md, at a 0.25 m fracture spacing, this was not very significant. Hence, these trends support our hypothesis that the incremental porosity and permeability were mainly dependent on the initial kerogen concentration of oil shale.

5. Comparative analysis

To validate the concept presented in this study, a comparative analysis of the results was also carried out and is presented in Table 4. The results of the study were compared with those of two previous studies by Kang [27] and Zhao [28]. The researchers carried out the incremental porosity evaluation of oil shale through laboratory experiments. Both of them used the oil shale samples from Fushun field of China. Fushun oil shale does not differ very much in organic composition from US Green River oil shale used in MDP. In our study, the kerogen consumption was estimated through numerical simulation, then the altered porosity was evaluated using the proposed model (Eq. (8)). The modeled incremental value of porosity of oil shale was in good agreement with the actual values of Fushun oil shale measured by Kang [27] and Zhao [28] through a series of laboratory experiments (Table 4).

Table 4. Comparative analysis of the results of this study with data of previous studies

Study	Oil shale field, location	Initial porosity, %	Tempera-ture, °C	Incremental porosity, %	Method
Kang [27]	Fushun, China	2.14	300	7.34	Conventional laboratory experiments
Current study	MDP, USA	5.00	340	12.50	Numerical and mathematical modelling
Kang [27]	Fushun, China	2.14	400	18.80	Conventional laboratory experiments
Zhao [28]	Fushun, China	2.14	400	20.33	Mercury intrusion laboratory experiments
Zhao [28]	Fushun, China	2.14	400	24.14	Computed tomography laboratory experiments

6. Conclusions

The study was conducted very carefully on the basis of extensive literature review, oil shale reservoir numerical simulation and mathematical modeling of the evaluation of incremental porosity and permeability. Based on the results of this research work the following conclusions are drawn:

1. By using the Green River oil shale data, considering the overburden-underburden heat losses, modifying the chemical reactions and modeling and lumping the hydrocarbon fluid components, the reservoir numerical simulation of oil shale was carried out.
2. On the basis of the in-situ kerogen conversion kinetics, a mathematical model for incremental porosity evaluation was established. The results demonstrated that porosity and permeability increased significantly during the in-situ conversion process of oil shale. The modeled values of porosity and permeability showed that their increment rate was mainly dependent on kerogen conversion.
3. Sensitivity analyses of the initial concentration of kerogen and fracture spacing were also performed. On the basis of the results of the sensitivity studies, it can be stated that the higher the initial concentration of kerogen, the greater the change in porosity and permeability.

Acknowledgments

This study was supported by the National Science Foundation (51674279, 51804328), Major National Science and Technology Project (2017ZX05009-001, 2017ZX05069, 2017ZX05072), Shandong Province Key Research and Development Program (2018GSF116004), Shandong Province Natural Science Foundation (ZR2018BEE008, ZR2018BEE018), Fundamental Research Funds for the Central Universities (18CX02168A), China Postdoctoral Science Foundation (2018M630813), Postdoctoral Applied Research Project Foundation of Qingdao city (BY201802003).

REFERENCES

1. Demirbas, A. Conversion of oil shale to liquid hydrocarbons. *Energ. Source. Part A*, 2016, **38**(18), 2698–2703. doi:10.1080/15567036.2015.1115925
2. Xu, Y., Sun, P., Yao, S., Liu, Z., Tian, X., Li, F., Zhang, J. Progress in exploration, development and utilization of oil shale in China. *Oil Shale*, 2019, **36**(2), 285–304. doi:10.3176/oil.2019.2.03
3. Dyni, J. R. *Geology and Resources of Some World Oil-Shale Deposits.* Scientific Investigations Report 2005-5294. US Geological Survey, Reston, Virginia, USA, 2006.

4. El-Mofty, S. E., Khairy, N., El-Kammar, A. M., El-Midany, A. A. Effect of mineralogical composition and kerogen content on oil shale natural floatability. *Energ. Source. Part A*, 2018, **40**(9), 1144–1152. doi:10.1080/15567036.2018.1474298
5. Fan, Y., Durlofsky, L. J., Tchelepi, H. A. Numerical simulation of the in-situ upgrading of oil shale. *SPE J.*, 2010, **15**(2), 368–381. doi:10.2118/118958-PA
6. Zafar, A., Su, Y. L., Wang, W. D., Alam, S. G., Khan, D., Yasir, M., Alrassas, A., Ahmad, I. Heat dissipation modeling of in-situ conversion of oil shale. *Open Journal of Yangtze Gas and Oil*, 2020, **5**(2), 46–53. https://doi.org/10.4236/ojogas.2020.52005
7. Zafar, A., Su, Y., Li, L., Mehmood, A., Wang, H., Fu, J. The numerical simulation and wellbore modelling of steam injection and stored heat recovery from light oil reservoir. *Energ. Source. Part A*, 2019. https://doi.org/10.1080/15567036.2019.1676331
8. Zafar, A., Su, Y., Wang, W., Li, L., Alam, S. G., Mehmood, A., Tahir, M. U., Fu, J. *The Numerical Simulation of Effects of Porosity, Permeability and Fluid Saturation on Heat Dissipation in an Oil Reservoir*. 2nd Conference of the Arabian Journal of Geosciences (CAJG), 25–28 November 2019, Sousse, Tunisia.
9. Wang, W., Fan, D., Sheng, G., Chen, Z., Su, Y. A review of analytical and semi-analytical fluid flow models for ultra-tight hydrocarbon reservoirs. *Fuel*, 2019, **256**, 115737. doi.org/10.1016/j.fuel.2019.115737
10. Zafar, A., Su, Y.-L., Li, L., Fu, J.-G., Mehmood, A., Ouyang, W.-P., Zhang, M. Tight gas production model considering TPG as a function of pore pressure, permeability and water saturation. *Pet. Sci.*, 2020, **17**, 1356–1369. https://doi.org/10.1007/s12182-020-00430-4
11. Zafar, A., Fan, H. J. Combination of geological, geophysical and reservoir engineering analyses in field development: a case study. *International Journal of Environmental, Chemical, Ecological, Geological and Geophysical Engineering*, 2017, **11**(1), 36–43.
12. Fan, H. J., Zafar, A., Alam, S. G., Kashif, M., Mehmood, A. Analyses of nature of fault through production data. *Open Journal of Yangtze Gas and Oil*, 2017, **2**(3), 176–190. https://doi.org/10.4236/ojogas.2017.23014
13. Wang, H., Su, Y., Wang, W., Sheng, G., Li, H., Zafar, A. Enhanced water flow and apparent viscosity model considering wettability and shape effects. *Fuel*, 2019, **253,** 1351–1360. doi.org/10.1016/j.fuel.2019.05.098
14. Lee, K. J. *Rigorous Simulation Model of Kerogen Pyrolysis for the In-situ Upgrading of Oil Shales*. PhD Dissertation, Texas A&M University, College Station, Texas, 2014.
15. Hazra, K. G., Lee, K. J., Economides, C. E., Moridis, G. *Comparison of Heating Methods for In-Situ Oil Shale Extraction*. 17th European Symposium on Improved Oil Recovery, From Fundamental Science to Deployment, 16–18 April 2013, Saint Petersburg, Russia. doi:10.3997/2214-4609.20142631
16. Bauman, J. H., Deo, M. D. Parameter space reduction and sensitivity analysis in complex thermal subsurface production processes. *Energ. Fuel.*, 2011,**25**(1), 251–259. doi:10.1021/ef101225g

17. Shen, C. *Reservoir Simulation Study of an In-Situ Conversion Pilot of Green-River Oil Shale*. SPE Rocky Mountain Petroleum Technology Conference, 14–16 April 2009, Denver, Colorado. doi:10.2118/123142-MS
18. Brandt, A. R. Converting oil shale to liquid fuels: energy inputs and greenhouse gas emissions of the Shell in situ conversion process. *Environ. Sci. Technol.*, 2008, **42**(19), 7489–7495. doi:10.1021/es800531f
19. Youtsos, M. S. K., Mastorakos, E., Cant, R. S. Numerical simulation of thermal and reaction fronts for oil shale upgrading. *Chem. Eng. Sci.*, 2013, **94**, 200–213. doi:10.1016.j.ces.2013.02.040
20. Jupp, T. E., Woods, A. W. Thermally driven reaction fronts in porous media. *J. Fluid Mech.,* 2003, **484**, 329–346. doi:10.1017/S0022112003004348
21. White, M., Chick, L., McVay, G. *Impact of Geothermic Well Temperatures and Residence Time on the In-Situ Production of Hydrocarbon Gases from Green River Formation Oil Shale.* 30th Oil Shale Symposium, Colorado School of Mines, Colorado Energy Research Institute, Golden, Colorado, USA, 18–20 October 2010, Presentation 7–1.
22. Bai, F., Sun, Y., Liu, Y., Guo, M. Evaluation of the porous structure of Huadian oil shale during pyrolysis using multiple approaches. *Fuel*, 2017, **187**, 1–8. doi:10.1016/j.fuel.2016.09.012
23. Han, J., Sun, Y., Guo, W., Li, Q., Deng, S. Characterization of pyrolysis of Nong'an oil shale at different temperatures and analysis of pyrolysate. *Oil Shale*, **36**(2S), 151–170. doi:10.3176/oil.2019.2S.06
24. Jia, J., Qian, R., He, J. Achieving resilience and sustainability through innovative design for oil shale pyrolysis process model. *Oil Shale*, 2019, **36**(2S), 142–150. doi:10.3176/oil.2019.2S.05
25. Liu, J., Liang, W., Kang, Z., Lian, H., Geng, Y. Study on the quantitative model of oil shale porosity in the pyrolysis process based on pyrolysis kinetics. *Oil Shale*, 2018, **35**(2), 128–143. doi:10.3176/oil.2018.2.03
26. Wang, L., Yang, D., Zhao, J., Zhao, Y., Kang, Z. Changes in oil shale characteristics during simulated in-situ pyrolysis in superheated steam. *Oil Shale*, 2018, **35**(3), 230–241. doi:10.3176/oil.2018.3.03
27. Kang, Z. *The Pyrolysis Characteristics and In-Situ Hot Drive Simulation Research That Exploit Oil-Gas of Oil Shale*. PhD Thesis, Taiyuan University of Technology, 2008 (in Chinese with English abstract).
28. Zhao, J. *Experimental Study on the Microscopic Characteristics and Mechanical Property of Oil Shale under High Temperature & Three-Dimensional Stress*. PhD Thesis, Taiyuan University of Technology, 2014 (in Chinese with English abstract).

Presented by Ma Yue
Received June 06, 2020